Video dehazing with spatial and temporal coherence

**Jiawan Zhang · Liang Li · Yi Zhang · Guoqiang Yang ·
Xiaochun Cao · Jizhou Sun**

Abstract This paper describes a new framework for *video dehazing*, the process of restoring the visibility of the videos taken under foggy scenes. The framework builds upon techniques in single image dehazing, optical flow estimation and Markov random field. It aims at improving the temporal and spatial coherence of the dehazed video. In this framework, we first extract the transmission map frame-by-frame using guided filter, then estimate the forward and backward optical flow between two neighboring frames to find the matched pixels. The flow fields are used to help us building an MRF model on the transmission map to improve the spatial and temporal coherence of the transmission. The proposed algorithm is verified in both real and synthetic videos. The results demonstrate that our algorithm can preserve the spatial and temporal coherence well. With more coherent transmission map, we get better refocusing effect. We also apply our framework on improving the video coherence on the application of video denoising.

Keywords Video dehazing · Markov random field · Image dehazing · Video enhancement

J. Zhang · L. Li (✉) · G. Yang · X. Cao · J. Sun
School of Computer Science and Technology, Tianjin University, Tianjin, China
e-mail: allen.liliang@gmail.com

J. Zhang · L. Li · Y. Zhang · G. Yang · X. Cao · J. Sun
MTS Lab, Tianjin University, Tianjin, China

J. Zhang · Y. Zhang
School of Software, Tianjin University, Tianjin, China

1 Introduction

The photographs and videos we get in our daily life are easily plagued by the aerosols suspended in the medium. The rays reflected by the objects' surfaces are not only attenuated by the aerosols but also blended with the *airlight* [14], which makes the image/video contrast lost and/or vividness lost.

As the degradation is spatial-variant, it is a challenge to recover the color and details of scene from the foggy images/videos. General contrast enhancement techniques, such as histogram equalization and gamma correction, may not generate satisfying results. Therefore, many methods, such as using multiple images [17, 19, 20] or additional information [13], have been proposed.

In the context computational photography, single image haze removal algorithms have made significant progress. Various methods [2, 8, 9, 11, 16, 22, 27] have been proposed based on a variety of priors or assumptions. The advantage of single image dehazing is that it needs minimal input and may be valid for most scenes. In Sect. 2 we will give a brief overview of these methods.

Compared to the extensive work on image dehazing, little work has been done on video dehazing. Extending image-dehazing algorithm to video is not a trivial work. The challenges mainly come from the following aspects:

– Computational efficiency. The algorithm must be able to efficiently process the large number of pixels in a video sequence. In particular, the user prefers less interaction and minimal input of data.
– Temporal coherence. It has been proven that human visualization system (HVS) is very sensitive to temporal inconsistencies presented in video sequences [24]. However, applying image-dehazing algorithm naively on

Fig. 1 Spatial inconsistency is (**a**) the foggy image, (**b**) the dehazed result using the method proposed in [23]. Note the rectangular region. Tarel's method [23] cannot well handle the region with discontinuous depth

Fig. 2 The foggy video and the results we get. (**a**) One frame in the original foggy video. (**b**) The dehazed frame

frame-by-frame often results in visual flicker. Figure 7 is an example of temporal coherence.

– Spatial consistency. The recovered video should be as natural as the original one. It is important to handle the inner-frame discontinuities in the video. Figure 1 shows the discontinuities in single-image dehazing.

In this paper, we present a method for restoring visibility from foggy videos, which can remove haze from videos and preserve the temporal and spatial coherence. We employ an efficient single-image-dehazing algorithm to perform per-frame processing to the foggy video, which outputs a sequence of transmission map of the original video. To improve the temporal coherence of the transmission map sequence, we leverage the optical flow techniques to find the corresponding pixels between neighboring frames. We generate forward and backward accuracy map to determine the accuracy of the flow field. Finally, based on the accuracy map, we utilize the *Gauss–Markov random field* to improve the spatial and temporal coherence of the transmission map. By the refined transmission map, we get a more visual coherent dehazed video. Figure 2 shows the result of our dehazing algorithm.

This paper is organized as follows. We begin by introducing the techniques our work built upon in Sect. 2. Then, we

describe our video dehazing algorithm in Sect. 3. In Sect. 4 we will show the results and compare our algorithm with that of the others'. We will also show other applications of our algorithm in Sect. 4. Finally, the limitations of our algorithm and the future work are given in Sect. 5.

2 Related work

In this section, we will introduce the work related to our algorithm, including single-image dehazing, optical flow estimation and temporal-spatial coherence improving.

Recently, single-image dehazing has made significant progress [2, 8, 9, 11, 16, 22, 27]. The success of these methods lies in a strong prior or assumption.

Many algorithms [11, 27] regard the transmission as a low frequency variable, i.e., assuming it varies smoothly in spatial domain. They either use Gaussian low-pass filter or assume the transmission is locally constant to get the crude transmission map and then refine it to get the final one.

Tan's work [22] is based on two observations. One is that clear-day images have more contrast than images plagued by bad weather; the other is that the variations of airlight, which mainly depends on the distance of objects to the viewer, tend to be smooth. Fattal [9] assumes that the transmission and the surface shading are locally uncorrelated. He et al. [11] propose Dark Channel Prior to solve the single-image-dehazing problem. Dong et al. [8] incorporate the sparse prior of nature image into the dehazing framework.

Optical flow is widely used in video processing [7]. It gives an estimation of the motion between the frames, which is quite useful for temporal coherence.

There are numerous methods to calculate optical flow. Baker et al. [3] give a modern survey of optical flow estimation. Efforts have been put into improving the optical flow constraints. Since the quadratic formulation is not robust to outliers, Black and Anandan [5] replaced the quadratic error function with a robust formulation. Haussecker and Fleet [10] proposed a physical constraint to model brightness change.

More recently, Xu et al. [25] provided a detailed preserving method, which can work well even when there are very small flow structures in the flow field. Although it achieves more accurate results, the complexity of the algorithm is very high, which makes it not very suitable for video processing.

In [21], Sun et al. uncover what has made the recent advances in the estimating optical flow by a thorough analysis of how the objective function, the optimization method influence accuracy. Besides, Sun et al. derive a new objective that formalizes the *median filtering* heuristics, which is a key to recent performance gains.

Markov Random Field (MRF) is quite useful for modeling spatial context and stochastic interaction among observ-
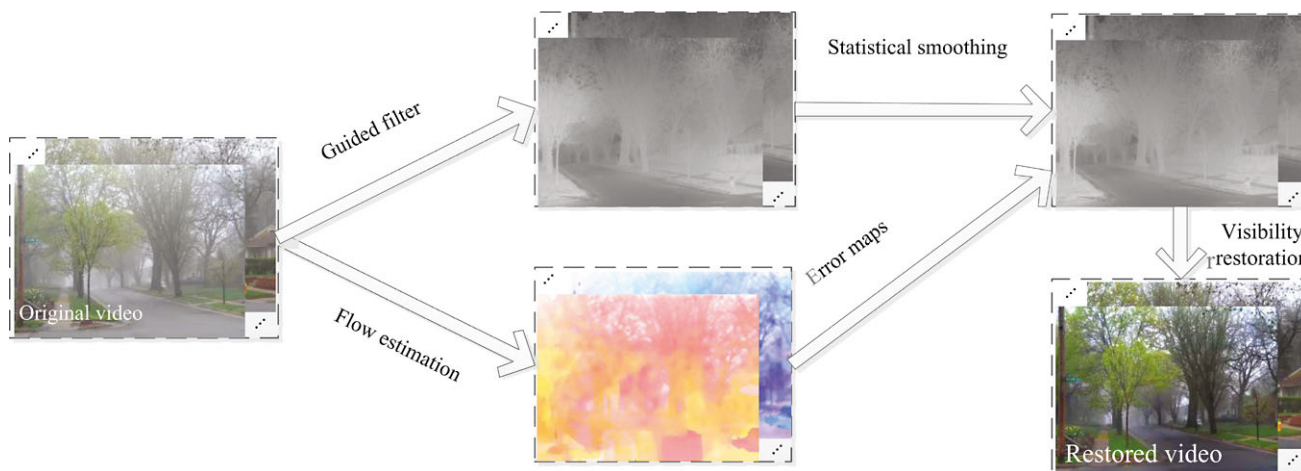
Fig. 3 Video dehazing flow chart. We first use guided filter to get the rough transmission map, then use the method proposed in [21] to estimate the corresponding pixels between neighboring frames. With the flow field, we get the forward and backward error maps. Based on the error maps, we build the MRF to proceed with a statical smoothing on the rough transmission map along temporal dimension. Finally, we restore the visibility using the refined transmission map to get the dehazed video

able quantities in many practical problems. As a result, MRF has generated a substantial amount of excitement in image processing, computer vision, and applied statistics.

In the context of video denoising, Chen and Tang [6] present a spatiotemporal MRF for video denoising. The MRF they constructed is based on a piecewise smoothness prior. The main advantage of the proposed MRF is that it integrates spatial and temporal information adaptively into a statistical inference framework. For image matting, Lin and Shi [15] proposed an MRF-based approach for image matting with complex scene. Fattal [9] used MRF to apply a statistical smoothing to the intermediate results.

3 Video dehazing

We incorporate the previously introduced techniques in our video dehazing framework. The flow chart of our framework is shown in Fig. 3.

The imaging model widely used for the foggy video is given by (1)[1]

$$\mathbf{I}(\mathbf{x}, s) = t(\mathbf{x}, s)\mathbf{J}(\mathbf{x}, s) + \big(1 - t(\mathbf{x}, s)\big)\mathbf{A}, \quad (1)$$

where $\mathbf{x}$ denotes the location of one pixel in frame s, $\mathbf{I}$ is the foggy video, $\mathbf{J}$ is the scene radiance in clear days, t is the medium transmission describing the portion of the light that is not scattered and reaches the camera, and $\mathbf{A}$ is the global atmospheric color. The goal of image restoration is to recover $t(\mathbf{x}, s)$, $\mathbf{J}(\mathbf{x}, s)$ and $\mathbf{A}$ for each pixel $\mathbf{x}$ in each frame s.

---

[1]The temporal dimension is denoted by s to differentiate between the transmission maps.

We assume the atmospheric color $\mathbf{A}$ is constant in the whole video, which makes it easy to estimate. Most image-dehazing algorithms estimate $\mathbf{A}$ from the pixels with highest intensities, which is fast but not accurate. For example, the brightest pixel maybe a white building or a white car. He et al. [11] integrate the airlight estimation with the dark channel prior and it makes the estimation result more accurate. Here we adapt the method they proposed.

Given the atmospheric color $\mathbf{A}$, we proceed with the following steps to restore the visibility of the foggy image.

3.1 Frame-by-frame dehazing

For each frame s, we first get the crude transmission map $\tilde{t}(\mathbf{x}, s)$ using dark channel prior

$$\tilde{t}(\mathbf{x}, s) = 1 - \omega \min_{c \in r, g, b}\left(\min_{\mathbf{y} \in \Omega(\mathbf{x})}\left(\frac{\mathbf{I}^c(\mathbf{y})}{\mathbf{A}^c} \right) \right), \quad (2)$$

where ω is a parameter for keeping some amount of haze for distant object, which is useful for some applications. As suggested in [11], the ω is fixed to be 0.95.

Then, we incorporate the *guided filter* [12] algorithm to refine the crude transmission map $\tilde{t}(\mathbf{x}, s)$. For each frame s, it assumes the refined transmission map $\mathring{t}(\mathbf{x}, s)$ is a linear transform of the foggy (guidance) image $\mathbf{I}(\mathbf{x}, s)$ in a window ω_x centered at pixel $\mathbf{x}$:

$$\mathring{t}(\mathbf{y}, s) = \mathbf{a}_x^{\mathrm{T}}\mathbf{I}(\mathbf{y}, s) + b_x, \quad \forall \mathbf{y} \in \omega_x, \quad (3)$$

where $\mathbf{a}_x$ and b_x are linear coefficients assumed to be constant in ω_x. To differentiate between the output $\mathring{t}(\mathbf{x}, s)$ and the input $\tilde{t}(\mathbf{x}, s)$ as little as possible, we minimize the follow-
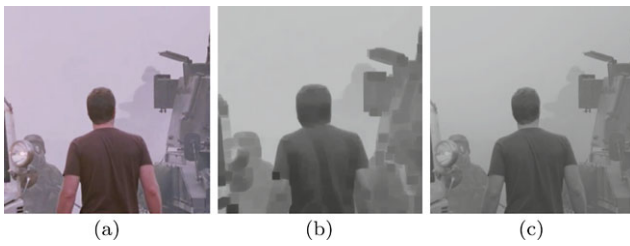
Fig. 4 Inner-frame processing. (**a**) 3rd frame of the original video **I**. (**b**) The crude transmission $\tilde{t}(\mathbf{x}, 3)$ taken from (2). (**c**) The refined transmission $\mathring{t}(\mathbf{x}, 3)$ using guided filter

ing cost function in the local window ω_x centered at pixel $\mathbf{x}$:

$$E(\mathbf{a}_x, b_x) = \sum_{\mathbf{y} \in \omega_x} \left(\left(\mathbf{a}_x^{\mathrm{T}} \mathbf{I}(\mathbf{y}, s) + b_x - \tilde{t}(\mathbf{x}, s) \right)^2 + \epsilon a_k^2 \right). \quad (4)$$

The small variable ϵ is a regulation parameter preventing $\mathbf{a}_x$ from being too large. The solution to (4) is given by

$$\mathbf{a}_x = (\Sigma_x + \epsilon \mathrm{U})^{-1} \left(\frac{1}{|\omega|} \sum_{\mathbf{y} \in \omega_x} \mathbf{I}(\mathbf{x}, s) \tilde{t}(\mathbf{x}, s) - \boldsymbol{\mu}_x \bar{t}(\mathbf{x}, s) \right), \quad (5)$$

$$b_x = \bar{t}(\mathbf{x}, s) - \mathbf{a}_x^{\mathrm{T}} \boldsymbol{\mu}_k,$$

where Σ_x is the 3×3 covariance matrix of $\mathbf{I}(\mathbf{x}, s)$ in ω_x, U is a 3×3 identity matrix, $\bar{t}(\mathbf{x}, s)$ is the mean value of the input $\tilde{t}(\mathbf{x}, s)$ in window ω_x and $\boldsymbol{\mu}_k$ is the mean vector of $\mathbf{I}(\mathbf{x}, s)$ in window ω_x.

By substituting (5) into (3), we get the refined transmission map $\mathring{t}(\mathbf{x}, s)$ for each frame. The result is shown in Fig. 4.

3.2 Optical flow estimation

Optical flow algorithm can be used to estimate the inter-frame motion at each pixel in a video sequence. For two neighboring frames, $\mathbf{I}(\mathbf{x}, s)$ and $\mathbf{I}(\mathbf{x}, s + 1)$, the most basic assumption made in optical flow calculation is image brightness constancy. In foggy image pair, the brightness of corresponding pixels is not exactly equal to each other due to the change of depth. Fortunately, the change is very tiny between two adjacent frames in a video. We regard that the brightness constraint is also valid:

$$\mathbf{I}(\mathbf{x}, s) \approx \mathbf{I}(\mathbf{x} + \mathbf{u}, s + 1), \quad (6)$$

where $\mathbf{u}$ describes the velocity of the pixel. To reduce the brightness difference in two frames, we perform pre-filtering as suggested in [5]. In our video dehazing process, we incorporated Sun's most recent optical flow estimation algorithm [21], for which an implementation is available on the author's web page.

In order to use optical flow to its fullest advantage, we follow the method proposed in [7]. For each frame s, we
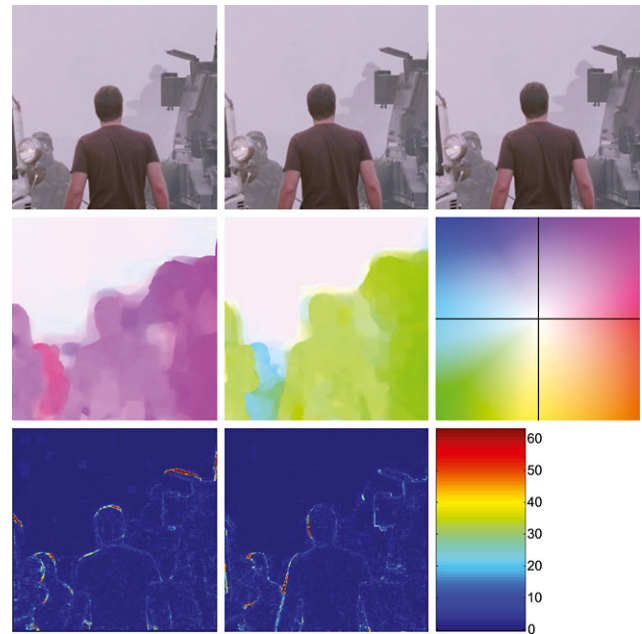
Fig. 5 Forward and backward error maps. *First row*: frame 3, 4, 5 of the original video. *Middle row*: forward flow field, backward flow field and *the color code* to draw the field. *Last row*: forward error map M_4^f and backward error map M_4^b

calculate two kinds of flow field, i.e. forward flow $\mathbf{u}_s^f$ from frame $s - 1$ to frame s and backward flow $\mathbf{u}_s^b$ from frame $s + 1$ to frame s. To determine the accuracy of these two flow fields, we create the forward error map M_s^f and the backward error map M_s^b. For a pixel $\mathbf{x}$ in frame s, the corresponding pixel in frame $s - 1$ is $\mathbf{x} - \mathbf{u}_s^f$ and in frame $s + 1$ is $\mathbf{x} - \mathbf{u}_s^b$. We compute the difference between the predicted color and the observed color in RGB color space,

$$M_s^f = \left\| I(\mathbf{x}, s) - I\left(\mathbf{x} - \mathbf{u}_s^f, s - 1\right) \right\|_2,$$
$$M_s^b = \left\| I(\mathbf{x}, s) - I\left(\mathbf{x} - \mathbf{u}_s^b, s + 1\right) \right\|_2, \quad (7)$$

where $\| \cdot \|_2$ is the L_2-norm of a vector. The forward and backward error maps give us a measure at each pixel of the accuracy of flow estimation from the previous and following frames. The error maps are shown in Fig. 5. We use this information to construct the MRF to improve the temporal coherence.

3.3 Temporal coherence improvement

With the assumption that the transmission of the corresponding pixels varies smoothly, we proceed with a statical smoothing along the temporal dimension using MRF to improve the spatial and temporal coherence of $\mathring{t}(\mathbf{x}, s)$, which is inspired by [9].

Fig. 6 The MRF model defined to improve the spatial and temporal coherence of the transmission map sequence
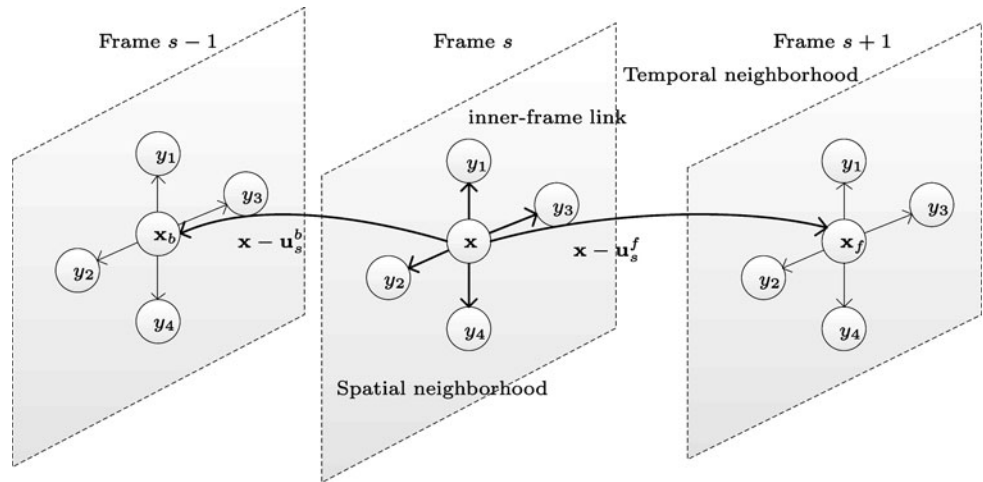
For a foggy video with n frames, the 3D MRF model is defined by (8):

$$P(t) \propto \prod_{s=1}^{n} \prod_{\mathbf{x} \in \mathbf{I}(\mathbf{x},s)} \exp\left(-\left(t(\mathbf{x},s) - \mathring{t}(\mathbf{x},s)\right)^2/\sigma_p^2\right)$$

$$\times \prod_{\forall \mathbf{y} \in \Omega_x} \exp\left(-P_s(\mathbf{x},\mathbf{y},s) \cdot \left(t(\mathbf{x},s) - t(\mathbf{y},s)\right)^2/\sigma_s^2\right)$$

$$\times \prod_{\forall c \in \{f,b\}} \exp\left(-P_t(\mathbf{x},c,s)\right.$$

$$\times \left(t(\mathbf{x},s) - t\left(\mathbf{x} - \mathbf{u}_s^c, s'\right)\right)^2/\sigma_t^2\right), \tag{8}$$

where Ω_x is the set of pixel $\mathbf{x}$'s four nearest neighbors in spatial domain, $\mathbf{u}_s^c$ is either $\mathbf{u}_s^f$ or $\mathbf{u}_s^b$. When $c = f$, then $s' = s - 1$ and when $c = b$, then $s' = s + 1$. $P_s(\mathbf{x},\mathbf{y},s)$ and $P_t(\mathbf{x},\mathbf{y},s)$ are the spatial and temporal priors, respectively. The spatial prior is defined as

$$P_s(\mathbf{x},\mathbf{y},s) = \frac{1}{(\mathring{t}(\mathbf{x},s) - \mathring{t}(\mathbf{y},s))^2}, \tag{9}$$

and the temporal prior is defined as

$$P_t(\mathbf{x},c,s) = \frac{1}{M_s^c(\mathbf{x})}, \quad \forall c \in \{f,b\}. \tag{10}$$

For each pixel $\mathbf{x}$ in frame s, $\mathbf{x} - \mathbf{u}_s^c$ is the corresponding pixel in frame s'. The first term in (8) defines the expectation of the final transmission map. The second term describes the spatial prior in each frame and the last one describes the temporal priors of adjacent frames. The link defined by (8) is illustrated in Fig. 6.

We maximize the probability by solving the linear system resulting from $d\log P/dt = 0$ and take this optimum to be our final transmission map.

Given the final transmission $t(\mathbf{x},s)$ for each frame, as suggested in [11], we recover the visibility using (11):

$$\mathbf{J}(\mathbf{x},s) = \frac{\mathbf{I}(\mathbf{x},s) - A}{\max(t(\mathbf{x},s),t_0)} + \mathbf{A}, \tag{11}$$

where t_0 is some lower bound to prevent the result from noise. Here we set $t_0 = 0.1$ in our experiments.

4 Results and comparison

In our experiments, we implement the guided filter using C++. For the linear system generated by MRF, we use Preconditioned Conjugate Gradient (PCG) algorithms as our solver. It takes about 30–40 seconds to get the transmission map for each frame using guided filter and 40–50 seconds to solve the large sparse linear equation for a 600×400 resolution 40-frame video on a PC with a 2.3 GHz Pentium Dual-Core processor.

We have conducted experiments on both synthetic and real foggy videos to test the proposed algorithm. First we compare our method with the frame-by-frame video dehazing algorithms. Figure 7 shows our result. Note for the leaves in the area marked with rectangular. The naive algorithm cannot preserve the temporal coherence while our algorithm preserves it well.

The evaluation of visibility restoration is difficult on real videos since no reference is available. So we synthesize a foggy video with "flat" fog, i.e. we assume the depth is a constant over the video, and then we restore the visibility of the synthetic video. We compare the *mean absolute difference* between consecutive frames of the dehazed video to show our algorithm can preserve the temporal coherence well. Figure 8 presents the results.

Applications The MRF model we proposed here can be used not only for restoring visibility but also for video de-
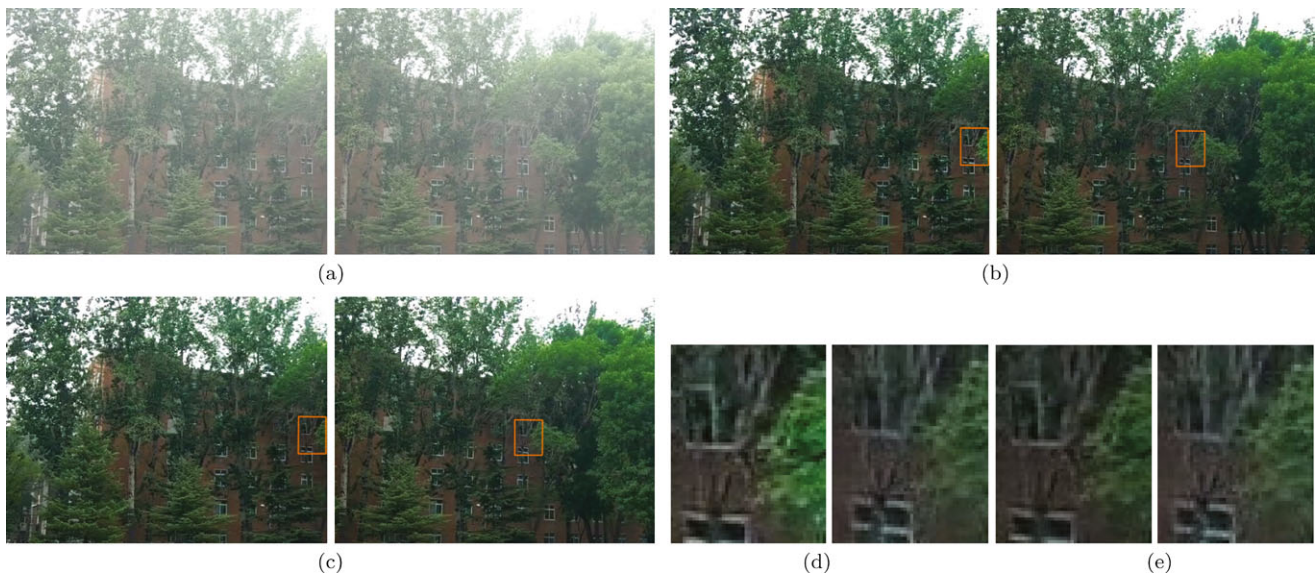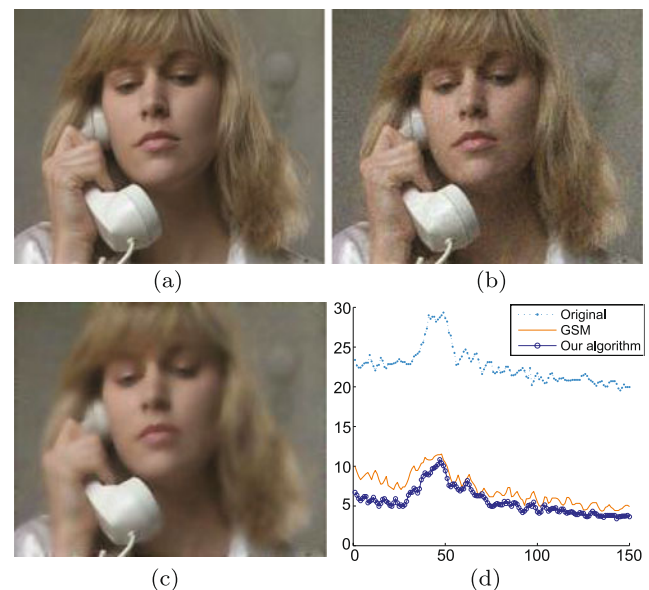
Fig. 7 Our results. (**a**) Two frames in a foggy video. (**b**) The results using the naive frame-by-frame method. (**c**) The results using our algorithm. (**d**) and (**e**) is the zoom of the rectangular region in (**b**) and (**c**). Note the leaves in the rectangular area. Frame-by-frame method cannot preserve the intensities of the leaves in neighboring frames unchanged
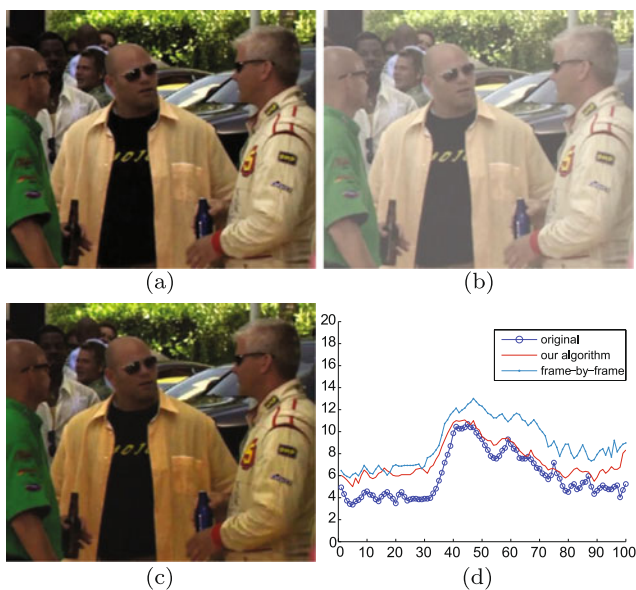
Fig. 8 Synthetic experiments. (**a**) The original sequence. (**b**) The result of adding the "flat" fog with constant $t = 0.6$. (**c**) The result of our dehazing algorithm. (**d**) The mean absolute difference of the original video, the naively frame-by-frame algorithm and our algorithm

Fig. 9 Application on video denoising. (**a**) Original frame taken from Suzie sequence [1]. (**b**) Noisy frames. The noise we added is the Gaussian white noise, with mean value $\mu = 0$ and standard variance $\sigma = 0.03$. (**c**) The denoised result using our algorithm. (**d**) The comparison of mean absolute difference

noising, video matting or other video processing. We just need to modify the spatial and temporal priors. Figure 9 is an example for video denoising. The videos we use are downloaded from [1]. We first denoise the video frame-by-frame using the Gaussian scale mixture (GSM) method, then build the MRF model on the denoised video to improve the temporal coherence. Figure 9(d) shows the result of comparing

of our algorithm with GSM. One can see from the mean absolute difference comparison that the sequence processed by our algorithm has much better coherence than the GSM method.

The predicted transmission map can be used for other applications on top of haze removal, such as changing the focus point of the video. Since the transmission map gains
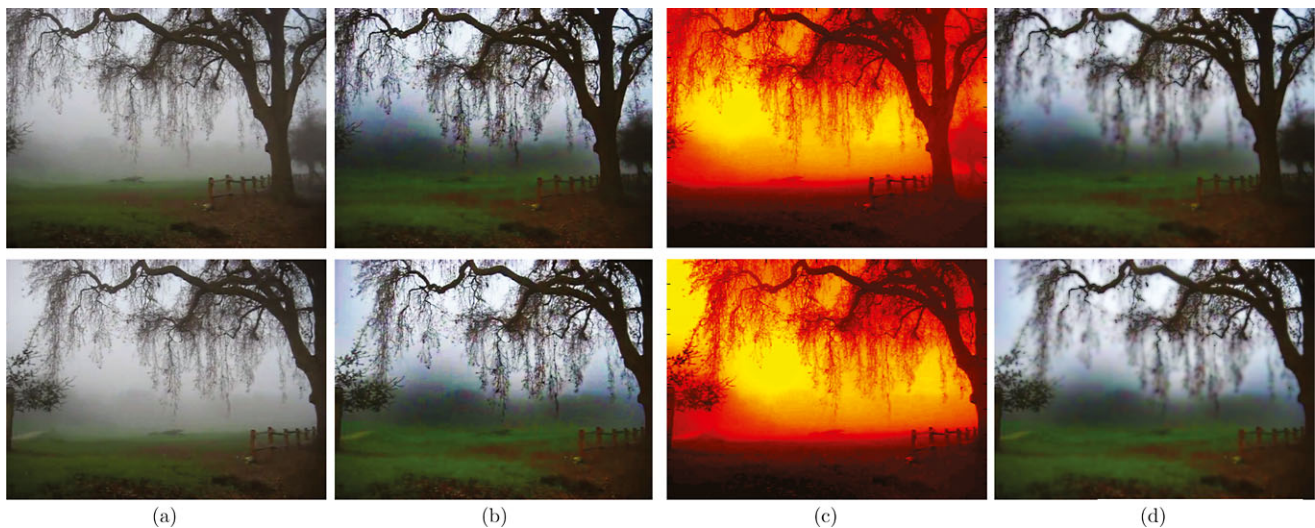
Fig. 10 The refocused effect. (**a**) The original frames. (**b**) Dehazed results using our algorithm. (**c**) Depth maps we get. (**d**) Refocused effects. In each frame, the focus plane is set on the tree

Fig. 11 The failure case. (**a**) The original image. (**b**) Transmission map recovered using dark channel prior. Since most of the scene is covered with snow, whose color is inherently similar to the atmosphere light, the transmission map is underestimated

Fig. 12 The scenes to the effect that the simple imaging model is not valid. A more complicated model [18] may be used to model these scenes

more temporal coherence, the effect of refocus is more smooth. Figure 10 shows our result of changing the focus plane.

5 Conclusion and future work

In this paper, we have proposed an algorithm to remove haze from a video while preserving the temporal and spatial coherence. We first apply guided filter to get transmission map for each frame. Then we proceed with a statical smoothing using MRF to smooth the transmission in temporal and spatial dimension.

Our algorithm only improves the coherence of the transmission map, while not making the result more exact. So it suffers from the same limitation as with dark channel prior. When the scene objects are inherently similar to the atmospheric light and no shadow is cast on them, the recovered transmission map is not accurate. The failure case is shown

in Fig. 11. Since the color of snow is similar to that of fog, the transmission of the snow is underestimated.

For future work, we intend to explore more constraints between frames, such as the geometry constraints proposed in [26]. Although it may be more computationally complex, the recovered result is more accurate.

The model we used may be invalid for complicated scene, such as the sun's influence on the sky region which is shown in Fig. 12. To deal with these scenes, more advanced model [18] can be used. We intend to investigate the haze removal based on these models in the future.

Besides, it is more computationally effective to solve the large sparse linear system in GPU. We plan to implement the sparse linear system solver on GPU [4] for the future work.

References

1. http://media.xiph.org/video/derf/ (2006). Xiph.org test media
2. Ancuti, C.O., Ancuti, C., Hermans, C., Bekaert, P.: Layer-based single image dehazing by per-pixel haze detection. In: ACM SIGGRAPH ASIA 2010 Sketches, SA '10, pp. 45:1–45:2 (2010)
3. Baker, S., Roth, S., Scharstein, D., Black, M.J., Lewis, J., Szeliski, R.: A Database and Evaluation Methodology for Optical Flow (2007)
4. Bolz, J., Farmer, I., Grinspun, E., Schröoder P.: Sparse matrix solvers on the GPU. ACM Trans. Graph. **22**, 917–214 (2003)
5. Black, M.J., Anandan, P.: The robust estimation of multiple motions: parametric and piecewise-smooth flow fields. Comput. Vis. Image Underst. **63**(1), 75–104 (1996)
6. Chen, J., Tang, C.K.: Spatio-temporal markov random field for video denoising. In: IEEE Conference on Computer Vision and Pattern Recognition (2007)
7. Chuang, Y.Y., Agarwala, A., Curless, B., Salesin, D.H., Szeliski, R.: Video matting of complex scenes. In: SIGGRAPH (2002)
8. Dong, X.M., Hu, X.Y., Peng, S.L., Wang, D.C.: Single color image dehazing using sparse priors. In: 2010 17th IEEE International Conference on Image Processing (ICIP), pp. 3593–3596 (2010)
9. Fattal, R.: Single image dehazing. ACM Trans. Graph. **27**(3), 1–9 (2008)
10. Haussecker, H.W., Fleet, D.J.: Computing optical flow with physical models of brightness variation. IEEE Trans. Pattern Anal. Mach. Intell. **23**, 661–673 (2001)
11. He, K., Sun, J., Tang, X.: Single image haze removal using dark channel prior. In: IEEE Conference on Computer Vision and Pattern Recognition, pp. 1956–1963 (2009)
12. He, K., Sun, J., Tang, X.: Guided image filtering. In: European Conference on Computer Vision (2010)
13. Kopf, J., Neubert, B., Chen, B., Cohen, M., Cohen-Or, D., Deussen, O., Uyttendaele, M., Lischinski, D.: Deep photo: model-based photograph enhancement and viewing. ACM Trans. Graph. **27**(5) (2008)
14. Koschmeider, H.: Theorie der horizontalen sichtweite. Beitr. Phys. D. Freien Atm., 171–181 (1924)
15. Lin, S.Y., Shi, J.Y.: A Markov random field model-based approach to natural image matting. J. Comput. Sci. Technol. **22** (2007)
16. Lv, X., Chen, W., Shen, I.F.: Real-time dehazing for image and video. In: Pacific Conference on Computer Graphics and Applications, pp. 62–69 (2010)
17. Narasimhan, S.G., Nayar, S.K.: Chromatic framework for vision in bad weather. In: Proceedings of the IEEE Computer Society Conference on Computer Vision and Pattern Recognition, vol. 1, pp. 598–605 (2000)
18. Preetham, A.J., Shirley, P., Smits, B.: A practical analytic model for daylight. In: ACM SIGGRAPH (1999)
19. Schechner, Y.Y., Narasimhan, S.G., Nayar, S.K.: Instant dehazing of images using polarization. In: Proceedings of the IEEE Computer Society Conference on Computer Vision and Pattern Recognition, Kauai, HI, United States, vol. 1, pp. I325–I332 (2001)
20. Shwartz, S., Namer, E., Schechner, Y.Y.: Blind haze separation. In: Proceedings—Conference on Computer Vision and Pattern Recognition, CVPR 2006, vol. 2, pp. 1984–1991 (2006)
21. Sun, D., Roth, S., Black, M.J.: Secrets of optical flow estimation and their principles. In: IEEE Conference on Computer Vision and Pattern Recognition (2010)
22. Tan, R.T.: Visibility in bad weather from a single image. In: IEEE Conference on Computer Vision and Pattern Recognition (2008)
23. Tarel, J.P., Hautière, N.: Fast visibility restoration from a single color or gray level image. In: Proceedings of IEEE International Conference on Computer Vision, Kyoto, Japan, 2009, pp. 2201–2208 (2009)
24. Villegas, P., Marichal, X.: Perceptually-weighted evaluation criteria for segmentation masks in video sequences. IEEE Trans. Image Process. **13**(8), 1092–1103 (2004)
25. Xu, L., Jia, J., Matsushita, Y.: Motion detail preserving optical flow estimation. In: IEEE Conference on Computer Vision and Pattern Recognition (2010)
26. Zhang, G., Jia, J., Wong, T.T., Bao, H.: Recovering consistent video depth maps via bundle optimization. In: IEEE Conference on Computer Vision and Pattern Recognition (2008)
27. Zhang, J., Li, L., Yang, G., Zhang, Y., Sun, J.: Local albedo-insensitive single image dehazing. Vis. Comput. **26**, 761–768 (2010)

Jiawan Zhang received the M.Sc. and Ph.D. degrees in Computer Science from Tianjin University in 2001 and 2004, respectively. Currently, he is Associate Professor at the School of Computer Software and Adjunct Professor at the School of Computer Science and Technology, Tianjin University. His main research interests are visual analytics, medical image processing, and image synthesis. He is a member of the ACM and IEEE.
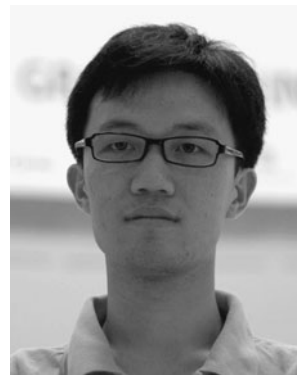
Liang Li received the B.Sc. degree at the School of Computer Science and Technology from Dalian University of Technology, P.R. China, in 2008. He is currently working towards the Ph.D. degree in Computer Application at the MTS Laboratory, Tianjin University. His main research interests include computer vision and information visualization.

Yi Zhang received M.Sc. and Ph.D. degrees in Computer Science from Tianjin University in 2006 and 2009, respectively. She is currently a lecturer in the School of Computer Software, Tianjin University. Her research interests include image editing techniques, virtual heritage restoration and information visualization.
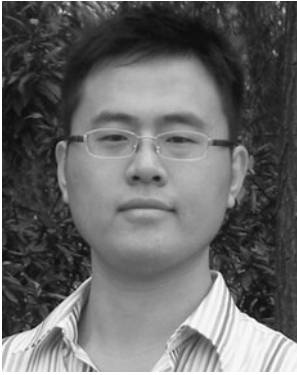
Guoqiang Yang Guoqiang Yang received the B.Sc. degree at the School of Computer Science and Technology from Hebei University of Technology, P.R. China, in 2008. He is currently working towards the M.Sc. degree in Computer Application at the MTS Laboratory, Tianjin University. His main research interests include computer vision and information visualization.

Xiaochun Cao received the B.E. and M.E. degrees, both in Computer Science, from Beihang University (BUAA), Beijing, China. He received the Ph.D. degree in Computer Science from the University of Central Florida, Orlando, USA, with his dissertation nominated for the university-level award for Outstanding Dissertation. After graduation, he spent about two and half years at ObjectVideo Inc. as a Research Scientist. Since August 2008, he has been with Tianjin Uni-versity, China, where he is currently a Professor of Computer Science. He has authored and co-authored over 40 peer-reviewed journals and conference papers, and has been in the organizing and the technical committees of several international colloquia. In 2004 and 2010, Dr. Cao was the recipients of the Piero Zamperoni best student paper award at the International Conference on Pattern Recognition.

Jizhou Sun Jizhou Sun received the M.Sc. degree from Tianjin University, China, in 1985 and the Ph.D. degree from Sussex University, U.K. in 1994. He is now a Professor in Computer Science and Technology in Tianjin University. His research interests include computer architecture, distributed and parallel computing, computer graphics process, virtual reality and network security.